

Atomistic simulations on adhesive contact of single crystal Cu and wear behavior of Cu-Zn alloy

You-Jun Ye(叶有俊), Le Qin (秦乐), Jing Li (李京), Lin Liu(刘麟)†, and Ling-Kang Wu(吴凌康) ‡

Citation: Chin. Phys. B, 2021, 30 (**2**): 026801. DOI: 10.1088/1674-1056/abbbf6
Journal homepage: http://cpb.iphy.ac.cn; http://iopscience.iop.org/cpb

What follows is a list of articles you may be interested in

Influence of external load on friction coefficient of Fe-polytetrafluoroethylene

Xiu-Hong Hao(郝秀红), Deng Pan(潘登), Ze-Yang Zhang(张泽洋), Shu-Qiang Wang(王树强), Yu-Jin Gao(高玉金), Da-Peng Gu(谷大鹏)

Chin. Phys. B, 2020, 29 (**4**): 046802. DOI: 10.1088/1674-1056/ab7da0

Indenter size effect on the reversible incipient plasticity of Al (001) surface: Quasicontinuum study

Tang Dan, Shao Yu-Fei, Li Jiu-Hui, Zhao Xing, Qi Yang

Chin. Phys. B, 2015, 24 (**8**): 086805. DOI: 10.1088/1674-1056/24/8/086805

First-principles calculations on Si (220) located 6H-SiC (10$\bar{1}$0) surface with different stacking sites

He Xiao-Min, Chen Zhi-Ming, Pu Hong-Bin, Li Lian-Bi, Huang Lei

Chin. Phys. B, 2014, 23 (**10**): 106802. DOI: 10.1088/1674-1056/23/10/106802

Peptide friction in water nanofilm on mica surface

Zhou Bo,Xiu Peng,Wang Chun-Lei,Fang Hai-Ping

Chin. Phys. B, 2012, 21 (**2**): 026801. DOI: 10.1088/1674-1056/21/2/026801

Atomistic simulations on adhesive contact of single crystal Cu and wear behavior of Cu–Zn alloy*

You-Jun Ye(叶有俊)[1], Le Qin (秦乐)[2,3], Jing Li (李京)[2], Lin Liu(刘麟)[2,†], and Ling-Kang Wu(吴凌康)[4,‡]

[1] *National Quality Supervision and Inspection Center of Pressure Pipe Components, Special Equipment Safety Supervision Inspection Institute of Jiangsu Province, Nanjing* 210036, *China*
[2] *School of Mechanical Engineering, Changzhou University, Changzhou* 213164, *China*
[3] *Jiangsu Power Equipment Co., Ltd, Changzhou* 213000, *China*
[4] *School of Material Science and Engineering, Georgia Institute of Technology, Atlanta, Georgia* 30332-0245, *USA*

(Received 12 July 2020; revised manuscript received 3 September 2020; accepted manuscript online 28 September 2020)

Atomistic simulations are carried out to investigate the nano-indentation of single crystal Cu and the sliding of the Cu–Zn alloy. As the contact zone is extended due to adhesive interaction between the contact atoms, the contact area on a nanoscale is redefined. A comparison of contact area and contact force between molecular dynamics (MD) and contact theory based on Greenwood–Williamson (GW) model is made. Lower roughness causes the adhesive interaction to weaken, showing the better consistency between the calculated results by MD and those from the theoretical model. The simulations of the sliding show that the substrate wear decreases with the mol% of Zn increasing, due to the fact that the diffusion movements of Zn atoms in substrate are blocked during the sliding because of the hexagonal close packed (hcp) structure of Zn.

Keywords: atomistic simulation, nano-indentation, wear behavior

PACS: 68.35.Af, 02.70.Ns, 68.35.–p, 73.43.Cd **DOI:** 10.1088/1674-1056/abbbf6

1. Introduction

In the past twenty years, micro-electro-mechanical systems (MEMSs) and nano-electro-mechanical systems (NEMSs) have exhibited enormous potential applications.[1] With excellent abrasion resistance and electrical conductivity, Cu and its alloys have great potential to be applied to MEMS and NEMS devices.[2] The contact and wear, which lead the device life to degrade, thus restricting the application of the Cu and its alloys in MEMS and NEMS. Moreover, contact and wear are the main sources of material loss on a nanoscale.[3,4] Therefore, the investigation of the contact and wear behavior for copper and its alloys on a nanoscale is one of the key approaches to optimizing the design and reduce the material loss of MEMS and NEMS devices.

As a classical contact model, the GW contact model is based on continuum theory to investigate the contact process, revealing the contact mechanism of the bonding surface on a microscale.[5] The GW model has been quite successful in describing contact behavior on a microscale.[6] The continuum theory is not well applicable for the contact behavior of discrete atomic systems at nanoscale.[7] In addition, for the basic mechanism of contact behavior on a nanoscale, no consensus has been reached. Therefore, revealing the contact mechanism on a nanoscale in depth is essential to exploring the complex phenomenon of the contact surfaces. Some novel experimental methods, such as nano-indentation, atomic force microscope (AFM), have been employed to investigate the friction process and wear mechanism on a nanoscale.[8] These experimental methods are not easy to analyze the characters of the atom, therefore the wear mechanisms on a nanoscale have not been understood well so far. As a novel analysis method, MD simulation is increasingly applied to atomic scale studies.[9–11] Considering the surface energy on an atomic scale, the contact and friction behavior exhibit size-dependent differences from on a macroscale. The atomistic simulation method is an effective method to explore the contact phenomena and wear mechanism on a nanoscale. Shen and Sun[12] conducted a series of MD simulations to delve into the friction behaviors of copper and diamond surfaces. Mojumder and Datta[13] studied the effect of copper percentage on the plasticity of Al–Cu alloy by the compressive load. However, the deformation and wear mechanism of Cu and its alloys, especially on a nanoscale, have not been fully explored.

In this study, the atomistic simulations are carried out to investigate the contact behavior of a single rough peak, in order to explore the fundamental mechanisms of contact behavior and the applicability of the theoretical model of single rough peak on a nanoscale. Additionally, the simulations of a diamond tip sliding against Cu–Zn alloy with different Zn content values (in mol%) are performed to investigate the effects

*Project supported by the National Key Research and Development Program of China (Grant No. 2018YFC0808800), the Natural Science Foundation of Jiangsu Higher Education Institutions, China (Grant No. 17KJA460002), and the "Six Talent Peaks" of Jiangsu Province, China (Grant No. GDZB-002).

†Corresponding author. E-mail: liulin@cczu.edu.cn
‡Corresponding author. E-mail: wumengling50@126.com

© 2021 Chinese Physical Society and IOP Publishing Ltd

of Zn atoms on wear behaviors.

2. Contact model of single rough peak

Under the micro contact assumption and with continuum theory, Greenwood[5] established the GW model that describes the linear relationship between normal load and contact area. On a microscale, a large number of rough peaks exist on the contact surface, which suggests that the real contact is comprised of a lot of single rough peaks that contact each other. Considering the randomness of interface phenomenon, Greenwood simplified the contact between two rough surfaces into the contact between a rough surface and a smooth rigid plane. When the two rough surfaces are in contact, the number of contact micro-bulges n can be obtained from

$$n = \eta A \int_d^\infty g(z)\,\mathrm{d}z, \tag{1}$$

where A is the nominal contact area, η is the micro-bulge density, z is the height distribution, and $g(z)$ is the probability density function of rough surface micro-bulges along with the height distribution.

The total contact area A_{sum} is calculated from

$$A_{\text{sum}} = \pi\eta AR\omega \int_d^\infty g(z)\,\mathrm{d}z, \tag{2}$$

where ω is the normal deformation of micro-bulge, R is the radius of the surface micro-bulge. The sum of contact load P_{sum} is obtained from

$$P_{\text{sum}} = \frac{4}{3}\eta AE^* R^{1/2}\omega^{3/2} \int_d^\infty g(z)\,\mathrm{d}z, \tag{3}$$

where E^* is the composite elastic modulus.[5]

From Eqs. (2) and (3) it follows that the relationship between the contact area A and the contact load P is a linear distribution, which is reasonable for the assumption and calculation due to the applicability of continuum theory on a macroscale and microscale. According to the assumption of GW model, some researchers made corrections to single rough peak.[14] During elastic contact and plastic contact, the contact area, and the contact force are as follows:

$$\begin{cases} A_{\text{e}} = \pi R^* \omega, \\ A_{\text{p}} = 2\pi R^* \omega, \\ A = A_{\text{e}} + A_{\text{p}}, \end{cases} \tag{4}$$

$$\begin{cases} F_{\text{e}} = \left[4E^* (R^*)^{1/2}\omega^{3/2}\right]/3, \\ F_{\text{p}} = 2\pi R^* \omega H, \\ F = F_{\text{e}} + F_{\text{p}}, \end{cases} \tag{5}$$

where A_{e} and F_{e} are the contact area and the contact force during the elastic contact, and A_{p} and F_{p} during the plastic contact; H is the Brinell hardness of soft material; R^* is the radius of the single rough peak. Based on Eqs. (4) and (5), for the single rough peak, the contact area A and the contact force F are both proportional to the normal deformation ω.[14]

It is questionable that the A is the contact area of the single rough peak. The actual contact area A_{real} is different from the A calculated by the continuum theory, thus the theory may not be applicable on a nanoscale. Moreover, it is difficult to obtain the atomic interaction of the contact interface experimentally. In this work, to better understand the interaction of the contact, MD simulations are employed to explore the nanoscale interface contact.

3. Simulation details

3.1. Initial configuration setup

The MD simulations are performed by using the large-scale atomic/molecular massively parallel simulator (LAMMPS). The atomistic models, which are for the single crystal copper and Cu–Zn alloy with 20 mol% of Zn, with a hemispherical diamond tip and plate substrate as shown in Fig. 1. The initial gap between the indenter tip and the substrate is 6.0 Å, which value is the vertical distance between the C atom at the bottom of the tip and the Cu/Zn atom on the surface of the substrate. Periodic boundary conditions are imposed along with the x and z directions and shrink-wrapped boundaries are implanted along the y direction. The x axis, y axis, and z axis are the orientation of [100], [010], and [001], respectively. The time step is 2.0 fs in the whole simulation, while the temperature is kept at 300 K to mimic the heat dissipation. During the nano-indentation and sliding simulation, the hemispherical diamond indenter tip is assumed to be rigid. The diamond indenter tip with a radius of 3.0 nm contains 1×10^4 atoms. The dimensions of the Cu–Zn substrate are 30 nm × 5 nm × 10 nm. For the alloy modeling, first, Cu atoms with different orientations are prepared, and then the part of Cu atoms are randomly replaced by Zn atoms with different content (in mol%). In the direction of the y axis, the substrate consists of three layers, *i.e.*, fixed layer, thermostat layer, and newton layer, which are shown in Fig. 1. The fixed layer with a thickness of 5 Å at the bottom of the substrate is

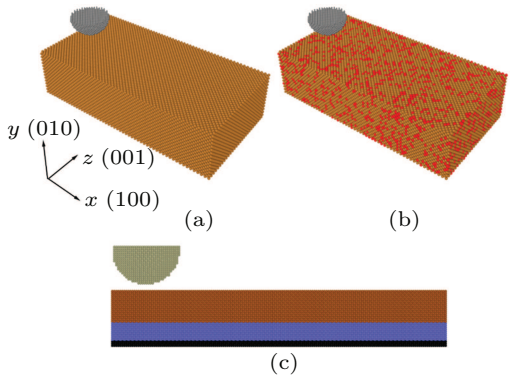


Fig. 1. Atomistic model of nano-indentation and sliding. Three-dimensional (3D) model the indenter tip of (a) diamond and (b) substrates of single crystal copper and Cu (brown)–Zn (red) alloy. (c) Two-dimensional (2D) view of atomistic model. Thermostat layer colored blue is adjacent to fixed layer colored black.

assumed to be frozen during simulations. The thermostat layer with a thickness of 15 Å is adjacent to the fixed layer. The temperature of the thermostat layer is fixed at 300 K by the Langevin thermostat baths. The atoms in Newton layer are unconstrained and move freely. The total number of substrate atoms is 135995.

3.2. Interatomic potential

The interatomic potential plays a key role in MD simulations. The potentials and relevant parameters are given in Table 1.[15–19]

Table 1. Parameters used in MD simulations.

Atomic pair	Parameters
C–C	rigid
Cu–Cu	EAM potential
Cu–C	Morse potential; $D_0 = 0.087$ eV, $\alpha = 5.14$ Å^{-1}, and $r_0 = 2.05$ Å^{-1}
Zn–C	Morse potential; $D_0 = 0.533$ eV, $\alpha = 3.28$ Å^{-1}, and $r_0 = 1.82$ Å^{-1}
Zn–Zn	MBMH potential; $A = 1.642 \times 10^{-9}$, $R = 0.29$, $Q = 4$, $\beta = 2.6$
Cu–Zn	LJ potential; $a = 0.025$, $R = 3.343$

The interaction among Cu atoms are described by the embedded atom method (EAM) potential as follows:

$$U = \sum_i F_i(\rho_i) + \frac{1}{2}\sum_{j\neq i}\varphi_{ij}(r_{ij}), \tag{6}$$

where F_i is the embedding energy, φ_{ij} is the pair potential term, and ρ_i is the electron cloud density generated by the extranuclear electrons of all the other atoms except atom i. It can be defined as

$$\rho_i = \sum_{j\neq i}\rho_j(r_{ij}), \tag{7}$$

where ρ_j (r_{ij}) is the charge density of extranuclear electrons of atom j, and r_{ij} is the distance between the atom i and the atom j. The parameters of EAM potential are developed by Foiles *et al.*[20]

The Born–Mayer–Huggins (MBMH) is used to model the interatomic interaction of Zn atoms as follows:[21]

$$U = A\exp\left(-\frac{r}{R_0}\right) - \frac{Q}{r}\exp\left(\frac{r}{\beta}\right), \tag{8}$$

where A is the Pauli factor, R_0 is the effective distance between atoms, Q is the number of charges, and β is the tunable parameter.

The interaction between Cu atom and Zn atom, modeled by Lennard–Jones potential, is shown below

$$U = D_0\left\{\left(\frac{R_0}{r}\right)^{12} - 2\left(\frac{R_0}{r}\right)^{6}\right\}, \tag{9}$$

where R_0 and D_0 are the empirical parameters, respectively.

Under the assumption of the rigid body for the indenter tip, the interactions among C atoms are neglected. In the absence of the chemical interactions, the Morse potential, which has been validated in simulations,[21–23] can account for the interaction between the substrate and the indentation tip as follows:

$$V(r) = a(\mathrm{e}^{-2\alpha(r-r_0)} - 2\mathrm{e}^{-\alpha(r-r_0)}), \tag{10}$$

where a is the binding energy parameter, α is the potential energy curve gradient coefficient, r and r_0 are the instantaneous and equilibrium distance between atoms, respectively.

3.3. Modeling methods

The simulations of the nano-indentation and sliding for the contact pair are detailed as follows. (i) The relaxation status is essential to ensuring that the system enters into the equilibrium. In addition, optimizing system energy and configuration make the substrate surface closer to the real material. The initial geometry of the alloy is relaxed sufficiently for 20 ps by using a canonical ensemble, or constant volume and temperature (NVT) ensemble. (ii) For the indentation simulation, due to the regular arrangement of single crystal copper, the relationship between the contact force and the indentation depth can be obtained by moving the indenter perpendicularly toward to the surface of single crystal copper substrate to investigate the contact on a nanoscale. The displacement loading, which allows for the decay of most of transient effects, is applied along the negative y direction at an indentation depth of 9.00 Å and a speed of 1 Å/ps. (iii) For the sliding simulation, after indentation process, with the indentation depth of 9.0 Å, the sliding processes are carried out. The substrates with 0, 5, 10, and 20 mol% of Zn are used along the x direction.

4. Results and discussion

4.1. Indentation of the single crystal copper

The evolution of the contact force with indentation time is illustrated in Fig. 2. From the curve it follows that the contact force is negative and appears at about 4 ps. The result suggests that it is an attractive force. Such a phenomenon is called adhesion.[24,25] As the tip approaches to the substrate, the macroscopic contact position is reached. Figure 2 shows the linear relationship between the contact force and the indentation time in the contact process.

Due to the effective radius of the atom, in the case of atomic scale the contact area, which is defined based on continuum theory on a macroscopic scale, is no longer applicable. A re-definition of contact area on a nanoscale was given in Ref. [26], and then a similar definition is used in this work.

In the GW model, the definition of the contact area is straightforward. The judgment of contact status is the positive repulsive force appearing on the contact surface. It is reasonable to take into account the assumed smooth surface. The assumed contact area is defined as the entire bonded surface, and moreover, the boundary of the contact area is enclosed by all

points, where the normal force decreases to zero.[26] However, adhesive interaction is ignored when the surface is assumed to be smooth. For the adhesive interaction, the normal force of the boundary does not decrease to zero directly. In contrast, the negative force is observed during 4 ps to 6 ps as shown in Fig. 2. As mentioned in Section 3, the gap between the intender tip and the substrate is 6 Å. Due to the indentation speed of 1 Å/ps, the y-axis coordinates are not equal at the time of 4 ps. Based on the definition of the GW model, the indenter tip does not contact the substrate while the attractive force is a negative value as shown in Fig. 2. However, the presence of a negative normal force indicates that the indenter tip and substrate are in contact on a nanoscale. Since the indenter tip and substrate are in contact status, the contact area needs exploring. Therefore, the re-definition of the real contact area on a nanoscale should be proposed.

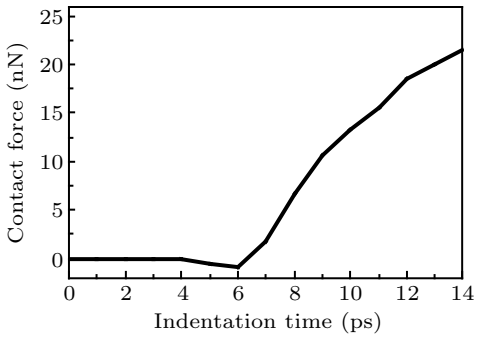


Fig. 2. Contact force *versus* indentation time.

In Ref. [26], the contact atoms between the contact surfaces are defined as the atoms that are in a finite range. The finite range is called the interactive radius, which is defined in the potential mentioned in Section 3 of this work. Based on the definition of contact status in GW model, two kinds of atoms, which are within the interactive radius and thus the normal force between them is negative, do not contact each other. During the simulation of the indentation process, when the atom on one surface is in the interactive radius of any atom on the other surface, the contact phase is considered on a nanoscale. In this status, each atom occupies a certain part of contact area. As shown in Fig. 3, the total contact area is the sum of the areas of all the contact atoms on the contact surface. It can be expressed as

$$A_{\text{real}} = N_{\text{atom}} \cdot A_{\text{atom}}, \tag{11}$$

where A_{real} is the contact area of total atoms, A_{atom} is the contact area of a single atom, and N_{atom} is the total number of atoms in the contact surface.

According to the Hertz theory and GW model, at the indentation depth in this research, the deformation is completely plastic.[5,14] Figure 4(a) shows the curves of the contact area *versus* indentation depth, which are obtained from the contact theory based on the GW model and MD simulation, respectively. In the case of a single rough peak, the curves show obviously the discrepancy between the theoretical model and the simulations. It can be seen that the contact area increases monotonically with indentation depth increasing. It is worth mentioning that the contact area obtained by the MD method is larger than that from the contact theory due to the adhesive interaction on an atomic scale. Furthermore, the relationship between the contact force and the indentation depth is shown in Fig. 4(b). It can be seen that the contact force increases with the growth of indentation depth, and similarly, the value of contact force calculated by MD simulation is larger than that calculated from the contact theory. The two results show significant discrepancy between contact scenarios on a nanoscale and on a macroscale.

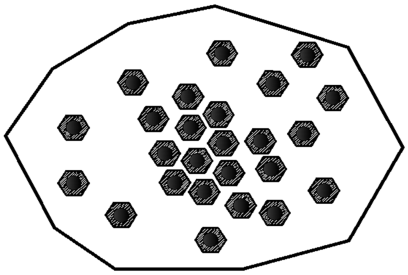


Fig. 3. Redefinition of contact area on a nanoscale. Dots colored black represent contact atoms on contact surface, and shadow area around contact atoms refers to contact area projected contact surface.

As no new definition for the contact force is available, the calculation method of the contact force in the contact theory is the same as that of in the MD simulation. The relationship between the contact force and the contact area is shown in Fig. 4(c). The MD results show a strong linear relationship with the contact theory results except for numerical difference. The discrepancy in contact force indicates the rationality of the redefinition for the contact area on a nanoscale. Due to the expansion of the contact area, the value of the contact force calculated by MD is higher than that by the contact theory. Moreover, it is worth noting that as shown in Figs. 4(a) and 4(b), neither the contact area nor the contact force rises linearly with indentation depth increasing any more. The results deviate from the results calculated from the contact theory.

For the GW model, the contact force and contact area both rise linearly with deformation increasing, whereas the results calculated by MD on a nanoscale show obvious differences in result between the theoretical model and the simulation. In this work, the adhesive interaction is considered in the indentation process. The process of normal force from negative to positive value illustrates the formation and extension of the contact zone. The results mean that because of adhesive interaction, the contact area calculated by MD is no longer the area encircled by the points where the normal force calculated by the theory model is zero. Therefore, the contact area calculated by MD is larger than that from the theoretical model.

In addition, the curve is sublinear and the trend of the curve becomes gentle with the increase of time. To further investigate the adhesive interaction between the contact surfaces on a nanoscale, the indentation simulations by using the indenter tips, respectively, with curvature radii of 10 Å, 30 Å, 50 Å, and 70 Å are carried out.

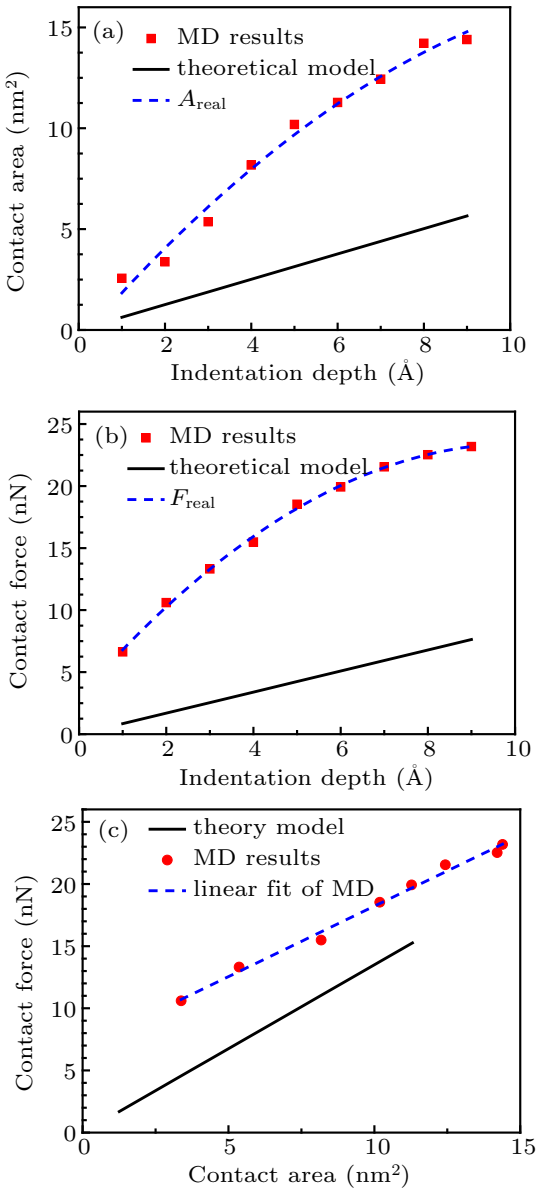


Fig. 4. (a) Contact area and (b) contact force *versus* indentation depth. (c) Contact force *versus* contact area.

The roughness of the contact surface drops with the radius of the indenter tip increasing.[26] Figures 5(a) and 5(b) show that the smaller surface roughness leads to more linear results. The parameter θ^2 is used to characterize the linearity of the curve. In Fig. 5(a), for indenter tips with the curvature radii of 10 Å, 30 Å, 50 Å, and 70 Å, the θ^2 values are 0.9364, 0.9783, 0.9938, and 0.9962, respectively. Similarly, the θ^2 values in Fig. 5(b) are 0.9159, 0.9202, 0.9603, and 0.9753, respectively. As the radius increases, θ^2 turns larger and the curve becomes more linear. Therefore, θ^2 is a parameter that measures the strength of adhesive interaction. Moreover, the adhesive interaction decreases with roughness increasing, indicating that the adhesive interaction is affected by surface roughness on a nanoscale. The lower the roughness of the contact surface is, the better agreement between the results of the MD and the theoretical model will be obtained.

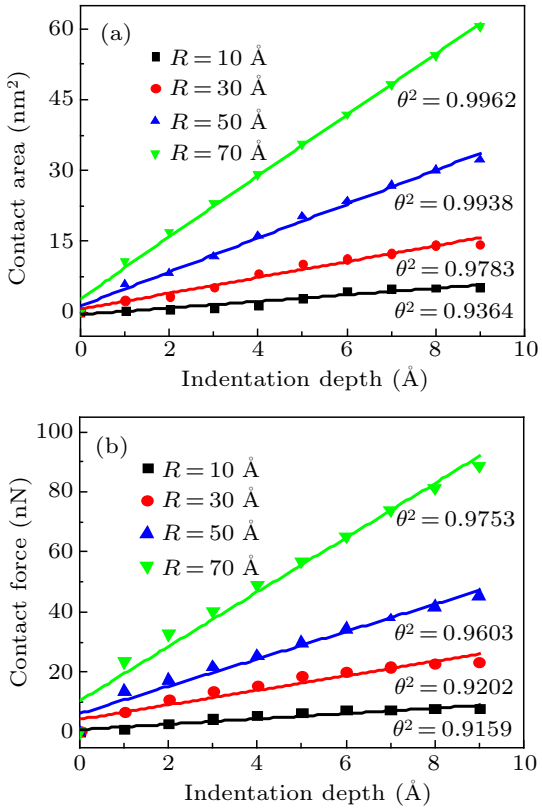


Fig. 5. Contact areas *versus* indentation depth with radii of 10 Å, 30 Å, 50 Å, and 70 Å, respectively, with parameter θ^2 denoting the linearity of curve.

4.2. Sliding of Cu–Zn alloy

After indentation process, the simulations of sliding are performed to investigate the Zn effect on wear behavior. The radius of the indenter tip and indentation depth are 30.0 Å and 9.0 Å, respectively. The friction coefficient is calculated as the friction force fluctuates around a fixed value. Figure 6 presents the friction coefficient and elastic modulus *versus* Zn content (in mol%) . The friction coefficient decreases with the Zn content rising in Fig. 6(a). Figure 6(b) shows the relationship between the elastic modulus and Zn content. It can be found that elastic modulus is proportional to Zn content. On a macroscale, according to the friction theory established by Bowden,[27] the elastic modulus is one of the main factors during the sliding. With the substrate is subjected to the shear from the indenter tip, higher elastic modulus means that the substrate can offset some part of shear force and then the friction force on the contact surface decreases.

Figure 7 shows the accumulating behaviors of substrate atoms, which are squeezed by the indenter tip, on the surface layer during the simulation. When the extrusion of atoms

reaches a certain extent, the atoms move out of the effect radius of contact atom, while the wear debris particles are generated. Referring to Shuai *et al.*'s statement.[28] for the definition of the lost atoms, the surface after the indenter tip sliding is shown in Fig. 7. Figure 8 exhibits the plots of total number (N) of lost atoms for the Cu–Zn alloy *versus* sliding time for the substrates with different Zn content (in mol%). The simulations indicate that the substrate wear decreases with Zn content increasing.

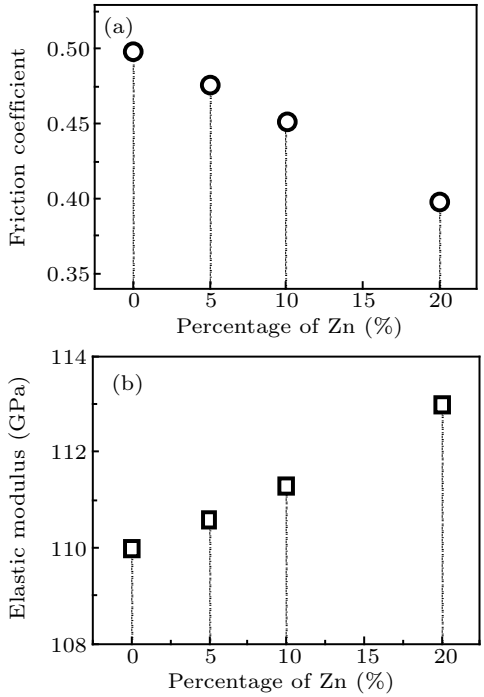


Fig. 6. (a) Friction coefficient and (b) elastic modulus *versus* Zn content.

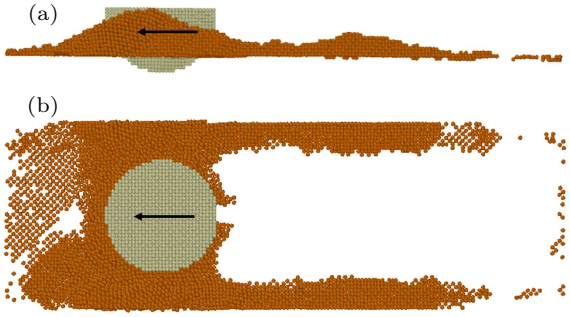


Fig. 7. Definition of lost atoms, showing (a) cross-sectional view and (b) top view, with sliding direction arrowed.

The anti-wear ability of Zn atoms is analyzed by the mean square displacement (MSD), which can be used to describe the diffusion behaviors of atoms. The formula is given as follows:[29]

$$r^2(t) = \frac{1}{N}\left\{\sum_{i=1}^{N}|r_i(t) - r_i(0)|^2\right\}, \tag{12}$$

where N is the total number of atoms for MSD calculation, $r_i(t)$ is the corresponding displacement of atom i at time t, and $r_i(0)$ refers to the initial displacement of atom i.

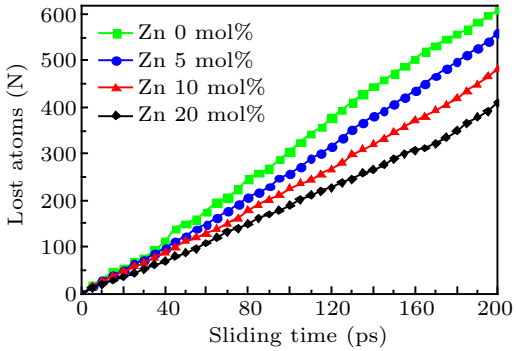


Fig. 8. Sliding-time-dependent total number of atoms lost from substrates with different Zn content.

Figure 9 shows the MSD results in all directions of Cu atoms in the surface layer. It can be seen that a large number of atoms are extruded out of the surface layer and tend to return to their original location, which leads the MSD results to fluctuate. Meanwhile, from the numerical results of MSD, we can also obtain the displacement of Cu and Zn atoms in the friction process. It is obvious that the substrate with higher Zn content exhibits lower MSD value, and the overall displacement of Cu atoms is greater than that of Zn atoms, which also suggests that Cu atoms move faster than Zn atoms. In other words, the substrates with higher Zn content are more stable. The atoms' combination is stronger in the substrate with higher Zn content. With the same shear force, the stronger combination leads the atoms in the surface layers to less move. For the substrates with higher Zn content, most of the energy produced by shear force is used to overcome the stronger combination between atoms, while the remaining energy converts into the kinetic energy of atoms to generate movement, which exhibits less diffusion and leads to lower MSD results.

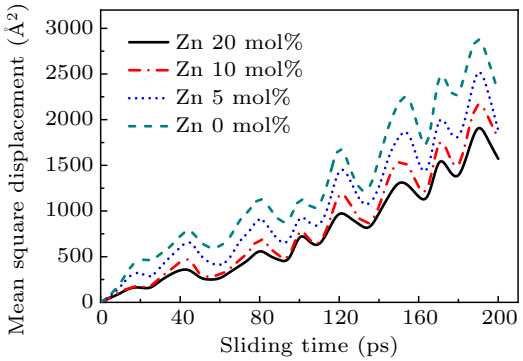


Fig. 9. Variations of MSD with sliding time for substrates with different Zn contents.

During the sliding, the MSD results of Cu and Zn atoms in the substrate with Zn content of 20 %mol are shown in Fig. 10. The MSD values of Cu atoms are much higher than those of Zn atoms at the same time points. It is illustrated that the Cu atoms have higher diffusion capability than Zn atoms. Comparing the diffusion of the Cu atoms with that of Zn atoms, the substrate structure is a face centered cubic (fcc) structure, where the Cu atoms are in self-diffusion. Meanwhile, Zn is of hcp structure, which blocks the Zn atoms from diffusing in

substrate. In the same condition, it needs more energy to pass over the potential barrier caused by dissimilar atoms, which means less energy converts into kinetic energy to generate movement. Briefly, in the same condition, the substrate with higher Zn content loses less atoms during sliding. In addition, higher elastic modulus and lower friction coefficient are observed in simulations, which reveal the anti-wear ability of Zn atoms in Cu–Zn alloy during sliding.

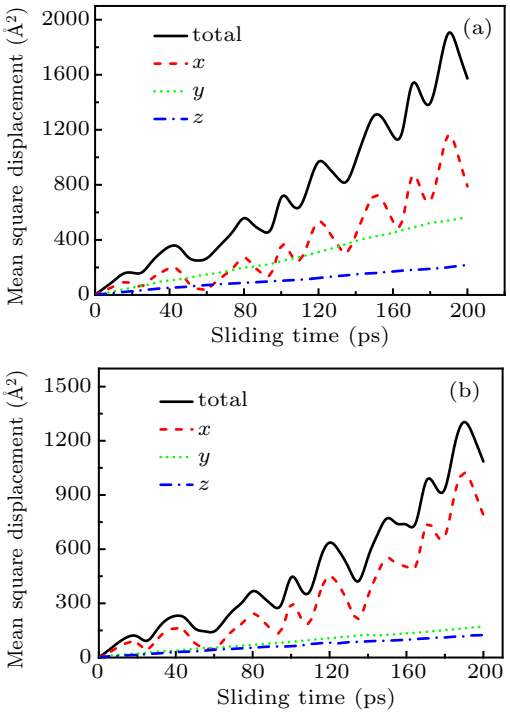


Fig. 10. Variations of MSD with sliding time for (a) Cu atoms and (b) Zn atoms.

5. Conclusions

Due to the adhesive interaction between the contacted atoms, the contact area and contact force calculated by MD are sublinear and deviate from those from the contact theory which is based on GW model. The effect of adhesive interaction decreases with roughness dropping. Lower roughness leads the calculated results from the MD and the theoretical model to be in better consistence.

The elastic modulus of the substrate increases with the Zn content rising, and the higher elastic modulus of the substrate can offset some part of shear force to reduce friction force on the contact surface. The Zn atoms can improve the atom combination of the substrate, thereby inhibiting the diffusion of the atoms. The anti-wear ability of Zn atoms is due to the (hcp) structure of Zn substance, which blocks the diffusion movements of Zn atoms in substrate.

References

[1] Zhao Y P, Wang L S and Yu T X 2003 *Journal of Adhesion Science and Technology* **17** 519
[2] Huang H, Li H, Wang A J, Zhong S X, Fang K M and Feng J J 2014 *Analyst* **139** 6536
[3] Raabe D, Miyake K and Takahara H 2000 *Mater. Sci. Eng. A* **291** 186
[4] Dupouy F, Snoeck E, Casanove M J, Roucau C, Peyrade J P and Askenazy S 1996 *Scr. Mater.* **34** 415
[5] Greenwood J A 1966 *Proc. Royal Soc. Lond.* **295** 300
[6] Luan B and Robbins M O 2006 *Phys. Rev. E* **74** 026111
[7] Jiang H Q, Hwang K C and Huang Y 2007 *Key Engineering Materials* **340** 11
[8] Ko H E, Park H W, Jiang J Z and Caron A 2018 *Acta Materialia* **147** 203
[9] Li Y, Li J H and Liu B X 2015 *Acta Materialia* **93** 105
[10] Adjaoud O and Albe K 2018 *Acta Materialia* **145** 322
[11] Li D, Wang F C, Yang Z Y and Zhao Y P 2014 *Sci. China- Phys., Mech. & Astron.* **57** 2177
[12] Shen B and Sun F 2009 *Appl. Surf. Sci.* **255** 7663
[13] Mojumder S and Datta D 2018 *Physica B* **530** 86
[14] Zhao Y, Maietta D M and Chang L 2000 *Journal of Tribology* **122** 86
[15] Yan Y D, Sun T, Dong S, Luo X C and Liang Y C 2006 *Appl. Surf. Sci.* **252** 7523
[16] Yan Y, Sun T, Dong S and Liang Y 2007 *Comput. Mater. Sci.* **40** 1
[17] Zhang J, Sun T, Yan Y and Liang Y 2009 *Mater. Sci. Eng. A* **505** 65
[18] Wang Z, Yubin W U and Hong Z 2008 *Mater. Rev.* **12** 103
[19] Bhattacharya B, Kumar G R D, Agarwal A, Erko A, Singh A and Chakraborti N 2009 *Comput. Mater. Sci.* **46** 821
[20] Foiles S M 1986 *MRS Proc.* **83** 889
[21] Shi J, Chen J, Fang L, Sun K, Sun J and Han J 2018 *Appl. Surf.* **435** 983
[22] Shi J, Chen J, Sun K, Sun J, Jing H and Liang F 2017 *Mater. Chem. Phys.* **198** 177
[23] Shi J, Zhang Y, Sun K and Liang F 2016 *Rsc Adv.* **6** 96824
[24] Neubauer E, Korb G, Eisenmenger-Sittner C, Bangert H, Chotikaprakhan S, Dietzel D, Mansanares A M and Bein B K 2003 *Thin Solid Films* **433** 160
[25] Sakami D, Lahmar A, Scudeller Y, Danes F and Bardon J P 2001 *J. Adhesion Science & Technology* **15** 1403
[26] Mo Y and Szlufarska I 2010 *Phys. Rev. B* **81** 035405
[27] Bowden F P 1951 *Am. J. Phys.* **19** 428
[28] Shuai X, Qiang W, Sha Z and Liu Z 2015 *Comput. Mater. Sci.* **110** 247
[29] Song C, Lin T, He P, Jiao Z, Tao J and Ji Y 2014 *Comput. Mater. Sci.* **83** 35